Journal of Advances in Medicine and Medical Research

30(9): 1-15, 2019; Article no.JAMMR.50994
ISSN: 2456-8899
(Past name: British Journal of Medicine and Medical Research, Past ISSN: 2231-0614, NLM ID: 101570965)

Cytotoxic Effects of Xanthohumol and Its Combination with Cisplatin on Human Metastatic Lung Cancer H1299 Cells

B. Long[1], E. Parks[1], P. Pacurari[2], A. Rieland[3] and M. Pacurari[1*]

[1]Department of Biology, College of Science, Engineering and Technology, Jackson State University, Jackson, MS, 39217, USA.
[2]School of Medicine, West Virginia University, Morgantown, WV, 26505, USA.
[3]School of Medicine, Howard University, Washington DC, USA.

Authors' contributions

This work was carried out in collaboration among all authors. Authors MP, BL, EP and PP conceptualized the study. Authors MP, BL, EP and AR did the methodology. Authors MP, BL, EP and AR did the analysis. Author MP did the resources. Authors MP, BL and EP prepared the original draft. Authors MP and PP did the writing-review and editing. Author MP supervised the study. Author MP performed the project administration. All authors have read and approved the final manuscript.

Article Information

DOI: 10.9734/JAMMR/2019/v30i930237
Editor(s):
(1) Dr. Muhammad Torequl Islam, Department of Pharmacy, Faculty of Life Science, Bangabandhu Sheikh Mujibur Rahman Science and Technology University, Gopalganj-8100 (Dhaka), Bangladesh.
Reviewers:
(1) Ibrahim Mohammed, Usmanu Danfodiyo University, Nigeria.
(2) Javier Camacho, Centro de Investigación y de Estudios Avanzados del Instituto Politécnico Nacional, Mexico.
(3) Martha Patricia Gallegos Arreola, Mexican Social Security Institute, Mexico.
Complete Peer review History: https://sdiarticle4.com/review-history/50994

Original Research Article

Received 02 July 2019
Accepted 06 September 2019
Published 19 October 2019

ABSTRACT

Aims: Non-small cell lung cancer (NSCLC) accounts for high lung cancer death that is mostly associated with advanced disease stage at diagnosis and resistance to chemotherapy. In the present study, we investigated whether xanthohumol, a prenylated flavonoid of hop plant, induces metastatic lung cancer H1299 cell death, and whether in combination with cisplatin there are additive effects.
Methodology: H1299 cells were grown and treated with xanthohumol (6.25, 12.5, or 25 μM), cisplatin (12.5, 25, or 50 μM) and the combination of cisplatin and xanthohumol for 24 h. Cell viability, cell morphology, chromatin condensation, ɣH2AX, cPARP-1, capsase-3, $p21^{WAF1/CIP1}$ and $p14^{ARF}$ genes were analyzed.

**Corresponding author: E-mail: maricica.pacurari@jsums.edu;*

Results: Xanthohumol, cisplatin, and the combination of cisplatin and xanthohumol inhibited H1299 cells viability. Cisplatin growth inhibitory effects were potentiated by xanthohumol. Xanthohumol induced chromatin condensation and apoptosis and potentiated cisplatin's effect vs cisplatin alone. Further investigation of growth inhibitory effects, xanthohumol alone induced γH2AX foci formation and the combination potentiated γH2AX foci formation. Cisplatin, xanthohumol at 25 μM, and the combination of cisplatin and xanthohumol at 6.25 and 12.5 μM increased cPARP-1 level. Active caspase-3 was increased by cisplatin, 12.5 μM of xanthohumol, and the combination of xanthohumol and cisplatin. Xanthohumol at 6.25 or 12.5 μM potentiated cisplatin effect on active caspase-3 and cPARP-1, respectively. Xanthohumol at 25 μM significtly induced the expression cell cycle control genes $p21^{WAF1/CIP1}$ and $p14^{ARF}$. These results indicate that xanthohumol inhibits proliferation of H1299 cells and induces cell death through cleavage of PARP-1 and activation of caspase-3. The combination of cisplatin and xanthohumol potentiated cytotoxic effects of each other compound.

Conclusion: The present study suggests that xanthohumol poses apoptotic effects and potentiates cisplatin's growth inhibitory effects on metastatic lung cancer cells.

Keywords: Metastatic lung cancer; plant; xanthohumol; cisplatin; combination; apoptosis; γ-H2AX; p21WAF1/CIP1; p14ARF.

1. INTRODUCTION

Lung cancer still remains the most common type of cancer worldwide. Moreover, the cancer of the lung and bronchus accounts for 27% of all cancer deaths and is the most common cause of cancer death in both sexes, men and women [1-2]. Lung cancer is a multifactorial disease with many risk factors [3]. Genetic, environmental and occupational factors, particularly, exposure to tobacco, non-ionizing and ionizing radiation, chemicals (asbestos, dioxins, metals, etc.), and industrial emissions are all high risk factors in lung cancer development [3]. Of all lung cancer types, non-small cell lung cancer (NSCLC) accounts for the highest number of lung cancer death [1-3]. The 5-year relative survival rate for localized and distant lung cancer is 18% and 4%, respectively [2]. The high NSCLC death rate is partly associated with advanced disease stage at diagnosis (metastasis) and resistance to chemo-drug cisplatin [2,4-6]. The exact mechanism by which cancerous cells overcome cisplatin therapeutic effects are not fully understood, however increased DNA repair and changes in the expression of genes regulating cell death are

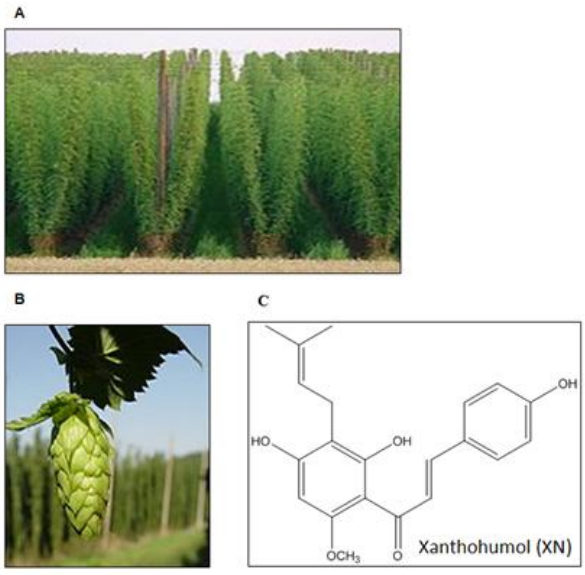

Fig. 1. Hops plant crop, Humulus lupulus (A), hops cone (B) and xanthohumol chemical structure (C). Xanthohumol is a prenylated chalcone found in the cone of hop plant [10-11]

suggested to play a role [6-8]. To overcome cisplatin resistance, new approaches are emerging such as combining cisplatin with other chemo-agents or natural plant extracts [8]. Mi et al. [6] showed that combining cisplatin with andrographolide, a natural diterpenoid, NSCLC were re-sensitized to cisplatin and tumor growth was inhibited through the activation of Akt/mTOR pathway and apoptosis. Similarly, Elkady et al. [9] showed that combining cisplatin with aqueous extract of cinnamon bark, cisplatin non-specific cytotoxicity was attenuated while its anticancer properties were preserved. Thus there is an interest in identifying phytochemicals that modulate biological properties of tumors. Xanthohumol (XN) is a prenylated flavonoid found in the flowers of hop plant *Humulus lupulus* L (Fig. 1) [10-11]. Studies have shown that xanthohumol exerts several biological properties including anti-angiogenic, anti-inflammatory, and anti-carcinogenic [10-12]. Slawinska-Brych et al. [13] showed that xanthohumol inhibited lung cancer cells growth through the inhibition of ERK pathway, up-regulation of cell cycle control genes, and activation of caspase-3. Similar results were reported in other cancer cells types including larynx cancer and multiple myeloma cells [14-16]. On metastatic colon cancer cells (SW620), xanthohumol has been shown to impair mitochondrial function and induce ROS production [15]. Yong et al. [16] tested xanthohumol effects on human lung adenocarcinoma cells (A549) and concluded that xanthohumol induced DNA fragmentation, cell arrest in the G1/S phase of cell cycle, and apoptosis. Studies have shown that advanced lung cancer treatment with chemotherapy is often presented with chemo-resistance and overcoming chemo-resistance still remains a challenge [17]. In the present study, we investigate cytotoxic effects of xanthohumol on metastatic lung cancer H1299 cells and whether xanthohumol potentiates cytotoxic effects of cisplatin.

2. MATERIALS AND METHODS

2.1 Chemicals

Xanthohumol was purchased from Sigma (St. Louis, MO). Caspase-3 assay and CyQUANT^{TM} NF cell proliferation assays were purchased from Invitrogen (Thermo Fisher Scientific, Grand Island, NY). Cisplatin was purchased from Acros (New Jersey) and a fresh stock solution (25 mM) prepared in PBS pH 7.4 Ca^{2+}/Mg^{2+} free that was further diluted in culture medium for cell treatments. Xanthohumol was prepared in DMSO according to methods previously described [10]. The stock solution of xanthohumol (50 mM) was kept at -20°C and used within 2 weeks. For cell culture studies, xanthohumol stock was further diluted to various concentrations in basal media before cell treatment thus achieving the final concentration of 0.1% DMSO.

2.2 Cell Culture

Human non-small cell lung cancer cell (NSCLC) line H1299 were purchased from the American Type Culture Collection (ATCC, Manassas, VA). Cell cultures were maintained in Dulbeco's Modified Medium (DMEM, ATCC) with 10% fetal bovine serum (FBS), and Streptomycin/ Neomycin (10,000/100 units, ATCC) in an incubator at 37°C, 5% CO2.

2.3 Cell Viability

Cell viability was measured using CyQUANT NF Assay according to manufacturer's protocol (Thermo Fisher Scientific). Briefly, the cells were subcultured in 96-well plates at a density of 10,000 cell/well in 10% FBS/DMEM/Penicillin/ Streptomycin (10,000/1000 units) for 24 h at 37°C/5% CO2. After 24 h, the media was changed to basal medium and the cells were treated with xanthohumol at 6.25, 12.5, 25, or 50 µM for 24 h. In some experiments, the cells were treated with cisplatin 12.5, 25 or 50 µM alone (ThermoFisher Scientific) or in combination with xanthohumol. After 24 h, the treatments were removed, and a fluorescent dye in binding buffer was added to each well and incubated for 50 min at 37ºC/5% CO2. After the incubation period, the absorbance was measure at 490/530 nm using a 96-well fluorescent microplate reader (SpectraMax 190, Molecular Scientifics, NH).

2.4 Cell Morphology

The cells were cultured in 6-well plates in 10%FBS/DMEM/Penicillin/Streptomycin for 24 h at 37°C/5% CO2. After 24 h, the cells were treated with xanthohumol 6.25, 12.5, or 25 µM, cisplatin 25 or 50 µM, and the combination of xanthohumol and cisplatin (25 µM) in basal media for 24 h. After 24 h, cell morphology micrographs were taken using phase-contrast inverted microscopy. Images were captured using a Carl Zeiss Axiovert 200 microscope equipped with Spot Camera.

2.5 Nuclear Staining by Hoechst 33258

The cells were seeded on cover slips in 6-well plates and allowed to adhere overnight. The cells were treated with various concentrations of xanthohumol for 30 h. At the end of the incubation period, the cells were fixed in 10% paraformaldehyde/PBS for 20 min at RT, and the plate spun down at 1000 rmp for 2 min, and washed with cold PBS. The cells were stained with Hoechst 33258 (10 µg/ml; Molecular Proves, NY) and incubated for 15 min at RT. The slides were examined and the apoptotic cells were identified according to the condensation and fragmentation of their nuclei observed under Olympus IX70 microscope (Olympus Optical Co., Ltd, Japan) equipped with a Retiga 2000R FAST camera (Qimaging, Canada). Images were acquired using SimplePCI software (Compix Inc., Sewickley, PA).

2.6 RNA Isolation

Total RNA was extracted using Trizol® (Invitrogen, CA) according to the manufacturer's protocol. To ensure a good RNA quality, the quality and integrity of the total RNA was evaluated using 28S/18S ratio and a visual image of the 28S and 18S bands were evaluated on the 2100 Bioanalyzer (Agilent Technologies, Santa Clara, CA). Concentrations of the total RNA were measured using the NanoDrop-1000 Spectrophotometer (NanoDrop Technologies, Germany).

2.7 Quantitative Real-time (q) PCR

For microRNA analysis, complementary DNA (cDNA) was generated using total RNA isolated as described above and according to the TaqMan Reverse Transcription protocol (Applied Biosystems Inc.). qPCR for cell cycle control genes $p21^{WAF1/CIP1,}$ $p14^{ARF}$, and 18S genes was performed using total RNA and cDNA was generated using a High-Capacity cDNA Reverse Transcription kit and TaqMan gene expression assays (Applied Biosystems Inc., CA). The levels of $p21^{WAF1/CIP1}$, $p14^{ARF}$, and 18S mRNA was measured using SYBR-Green Master mix and gene specific primers according to manufacturer's protocol (Applied Biosystems Inc.). All qRT-PCR reactions were performed on 7500 instrument (Applied Biosystems Inc.). In the qRT-PCR analysis of genes, the dissociation curve showed the absence of a secondary peak, indicating no presence of primer dimer. The expression level of each gene was determined by following formulas: fold change = $2-\Delta\Delta Ct$, where ΔCt (cycle threshold) = $Ct_{target\ gene}$ - $Ct_{endogenous\ control\ gene}$, and $\Delta\Delta Ct = \Delta Ct_{treated\ sample} - \Delta Ct_{control\ sample}$. 18S was used as an endogenous control gene [19-20].

2.8 Western Blot

After treatments, the cells were lysed in 1X SDS lysis buffer (50 mM Tris-HCl, pH 6.8, 2% SDS, 10% glycerol). Total protein was quantified by the BCA method. β-mercaptoethanol was added to lysates at a final concentration 100 mM. Equal amounts of total protein were separated by 4-12% SDS-PAGE and transferred to PVDF membranes. Membranes were blocked with 5% non-fat milk in 1X PBS containing 0.05% Tween-20 for 1 h at room temperature. Membranes were incubated with PARP primary antibody (Cell signaling) at 4ºC overnight. After the incubation, the membranes were washed three times in 1X PBS with 0.05% Tween-20 for 10 min and then incubated for 1 h at room temperature with horseradish peroxidase (HRP)- conjugated goat anti-mouse IgG in 5% non-fat milk/1X PBS/ 0.05% Tween-20. Membranes were then washed five times for 10 min in 1X PBS with 0.05% Tween-20. Proteins bands were visualized using an ECL Chemiluminescence Kit (Millipore, MA). Relative protein levels were normalization to control samples.

2.9 Ɣ-H2AX

ɣ-H2AX phosphorylation was analyzed using immunofluorescence [20,23]. Briefly, the cells were grown on cover slips and treated with xanthohumol (6.25, 12.5, or 25 µM), cisplatin (25 µM) or combination of xanthohumol (6.25, 12.5, or 25 µM) and cisplatin (25 µM) for 24 h. After the treatments, the cells were fixed in 4% paraformaldehyde for 20 min at RT, rinsed with ice-cold PBS (pH 7.4, $Ca^{2+/}Mg^{2+}$ free), and permeabilized in 0.1% Triton X-100/PBS for 20 min at RT. Cells were rinsed with PBS (2 times) and then incubated with 5% bovine serum albumin (BSA)/PBS/0.1% TritonX-100 for 2 h at RT and then incubated with anti-phosphorylated ɣH2A antibody (Thermofisher Scientific, Carlsbad, CA) in 5% BSA/PBS/0.1%Triton X-100 at 1:500 dilution overnight at 4ºC. After primary incubation, the cells were washed three times with PBS and then incubated with an Alexa-Fluor®-488-conjugated secondary anti-body (Molecular Probes, Life Technologies, MA)/5% BSA/PBS/0.1% TritonX-100 at a dilution of 1:1000 for 1 hour in the dark. After the secondary

antibody incubation, the cells were washed with PBS three times for 5 min each time, and mounted on slides with a mounting antifade solution containing DAPI (Molecular Probes, Eugene, OR). Images were captured with an Olympus epifluorescence microscope (Center Valley, PA).

2.10 Human Caspase-3 (Active) ELISA Assay

Active caspase-3 was measured using human caspase-3 ELISA assay from Invitrogen (ThermoFisher Scientific) according to manufacturer's protocol. Briefly, the cells were seeded in 6-well plates in normal growth media. After 24 h, the media was replaced with basal media and the cells were treated with xanthohumol (6.25, 12.5, 25 µM), cisplatin (25 µM), and the combination of cisplatin (25 µM) and xanthohumol (6.25, 12.5, or 25 µM) for 24 h. After 24 h, the media was removed, the cell monolayer was rinsed with PBS Ca^{2+}/Mg^{2+} free (4ºC) and lysed with 200 µL of cell lysis buffer containing protease inhibitor cocktail (Sigma). The level of active caspase-3 was measure according to manufacturer's protocol (ThermoFisher Scientific). Absorbance was measured at 490 nm using a plate reader (SpectraMax 190, Molecular Scientifics, NH).

2.11 Statistical Analysis

Data are presented as mean ± SEM from three experiments. Statistical analysis was performed using one-way analysis of variance (ANOVA) and Student's paired *t*-test with a significance level of $p \leq 0.05$ versus non-treated control samples.

3. RESULTS

3.1 Xanthohumol Decreases H1299 Cell Viability

The effect of xanthohumol on the proliferation of H1299 cells was determined using CyQuant assay. The H1299 cells were treated with 12.5, 25, or 50 µM of cisplatin, 6.25, 12.5, or 50 µM of xanthohumol, and a combination of cisplatin (25 µM) and 6.25, 12.5 and 25 µM of xanthohumol for 24 h (Fig. 2). Cisplatin, xanthohumol, and the combination of cisplatin (25 µM) and xanthohumol (6.25, 12.5 or 25 µM) significantly decreased cell viability compared to control (Fig. 2, * $p \leq 0.05$). Cisplatin anti-growth effects were potentiated by xanthohumol compared to 25 µM cisplatin alone (Fig. 2, # $p \leq 0.05$).

3.2 Xanthohumol Induces Cell Morphology Changes

The effect of different concentrations of xanthohumol on cell morphology were analyzed using light microscopy. At 6.25 µM, xanthohumol did not induce profound cell morphology changes compared to control cells, although some cells displayed vesicles (broken arrow) and mild shrinkage (Fig. 3, arrow). At concentrations higher than 6.25 µM, xanthohumol induced strong morphological changes such as cell-size shrinkage and formation of visible vesicles, and rounding (Fig. 3). At the highest tested concentration of 25 µM, xanthohumol induced profound cell rounding, shrinkage, and a reduction in cell number (Fig. 3, arrow). Combination of cisplatin (25 µM) and xanthohumol induced minimal cell rounding at 6.25 µM of xanthohumol. A greater cell morphological changes such as shrinkage and rounding were observed at 12.5 and 25 µM of xanthohumol in combination with cisplatin (25 µM) (Fig. 3, arrow and broken arrow).

3.3 Xanthohumol Effect on Nuclear Chromatin

The effect of xanthohumol on nuclear chromatin was analyzed following treatment of cells with different concentrations of xanthohumol (Fig. 4). Chromatin changes were determined using nuclear staining dye, Hoechst 33258, and the cells were examined using fluorescence microscopy. Cells treated with different concentrations of xanthohumol displayed nuclear chromatin changes such as chromatin condensation which fluoresced bright blue (arrow), whereas control cells stained dark blue and displayed a normal, round, and unpunctuated nucleus (Fig. 4A). The cells treated with xanthohumol showed condensed and fragmented nuclei which displayed bright blue fluorescent appearance compared to control, and these cells were scored as apoptotic cells (Fig. 4A, arrow). Xanthohumol significantly increased the number of apoptotic cells at concentrations higher than 6.25 µM compared to control (Fig. 4B). Cisplatin (25 µM) significantly induced apoptosis compared to control. Addition of xanthohumol to cisplatin significantly potentiated cisplatin's apoptotic effect compared to control and cisplatin alone (Fig. 4B).

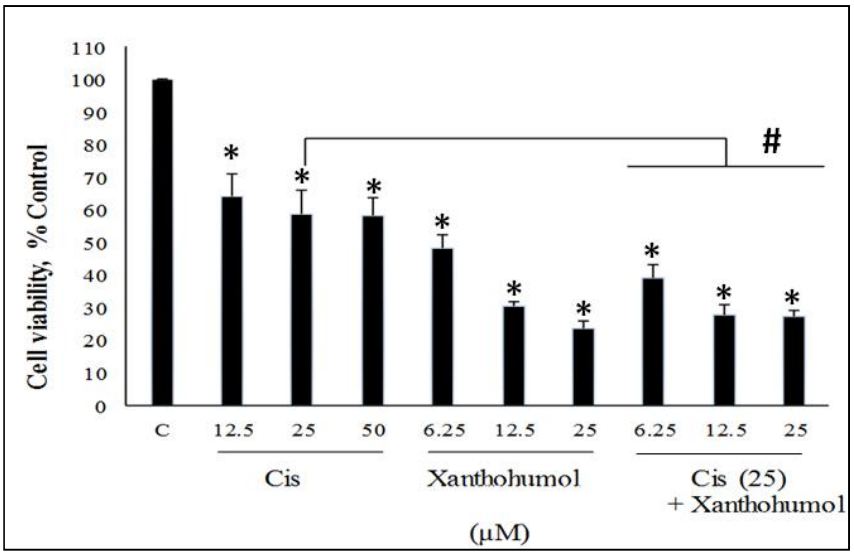

Fig. 2. Xanthohumol's effects on H1299 cells viability

*The cells were treated with different concentration of cisplatin, xanthohumol and combination of cisplatin (25 μM) and xanthohumol as shown in the figure for 24h. Cell viability was measure using CyQuant assay as described in Materials and Methods. Data is presented as % cell viability relative to control, n = 3. *, # Statistically significant, ANOVA, t-test, * p ≤ 0.05 vs control, and # p ≤ 0.05 vs 25 μM of cisplatin*

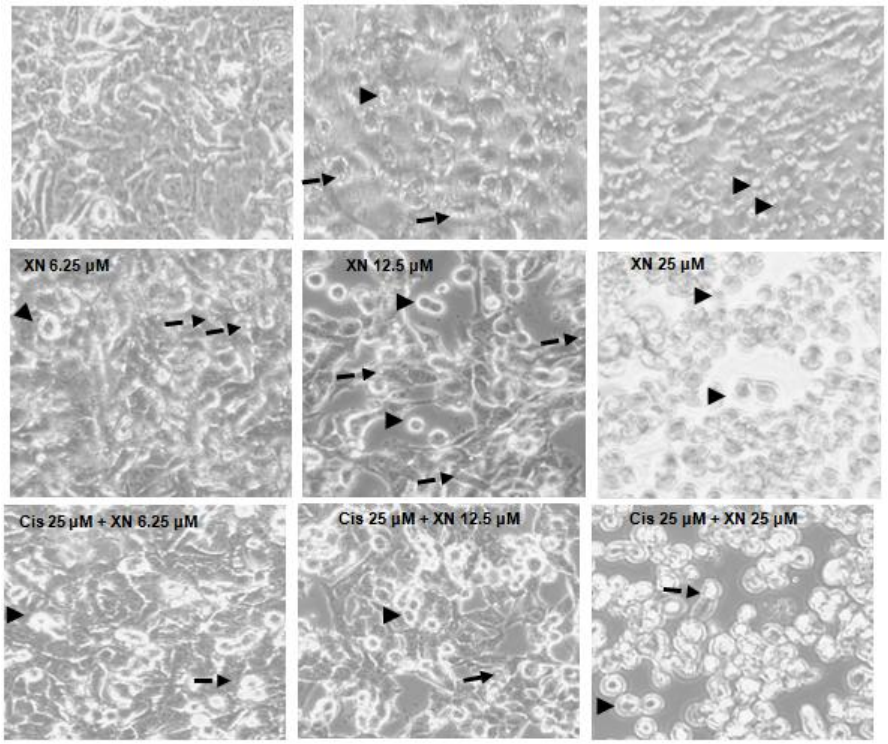

Fig. 3. Cell morphology changes in the absence and presence of cisplatin, xanthohumol, or combination of cisplatin and xanthohumol

The cells were seeded in growth media for 24 h followed by treatment with cisplatin, xanthohumol and combination of cisplatin and xanthohumol at different concentrations (μM) as shown in the figure for 24 h. Representative micrographs of one experiment are shown, n = 3. The micrographs were recorded using an inverted phase-contrast light microscope. Dotted arrow = cytoplasmic vacuoles; arrow head = cell rounding

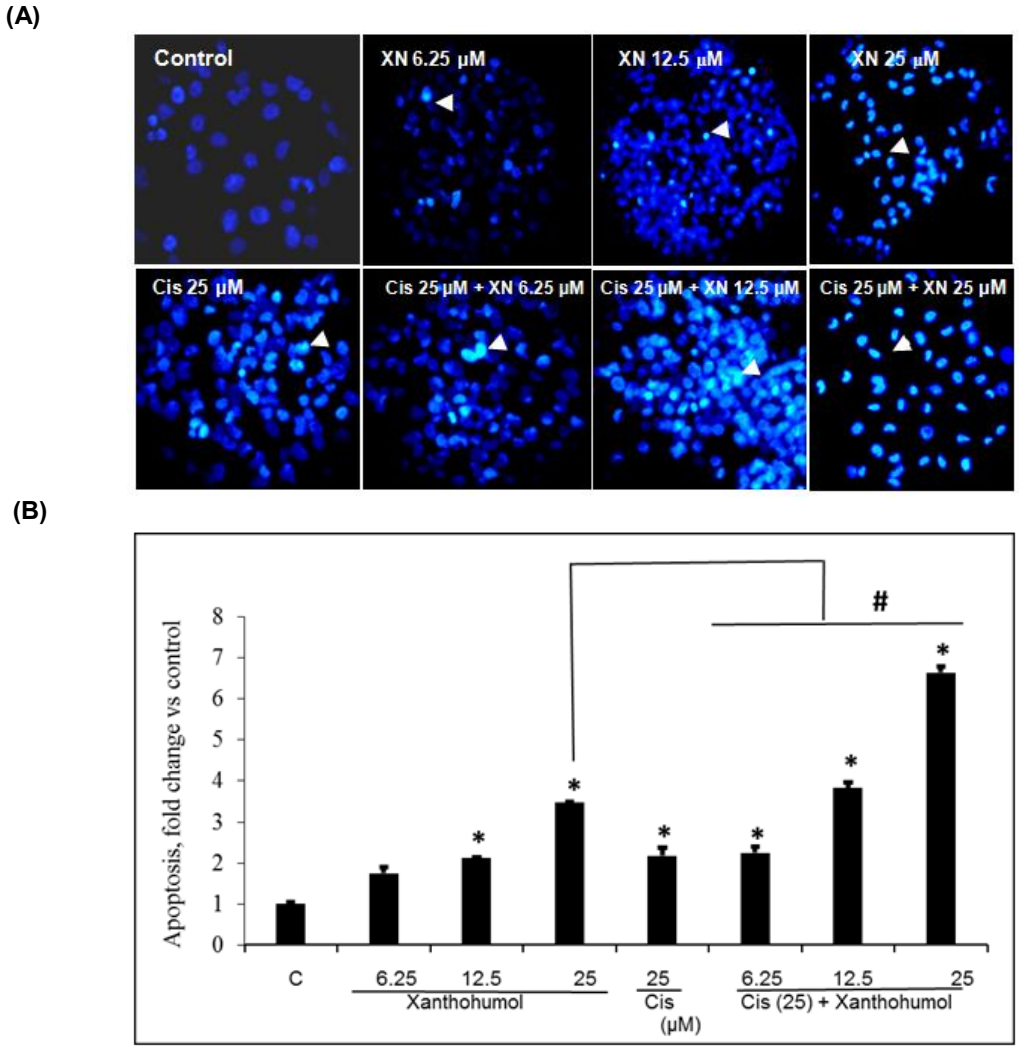

Fig. 4. The effect of xanthohumol on nuclear morphology

The cells were cultured on cover slips in growth media for 24h then treated with different concentrations of xanthohumol, cisplatin (Cis) and the combination of Cis and xanthohumol for 24h and shown in the figure. After treatments, the cells were washed, fixed, and stained with Hoechst 33258 and analyzed as described in Materials and Methods. A) The micrographs were taken with a fluorescent microscope. One representative micrograph is shown, n = 3. The arrow indicates condensed chromatin and condensed nuclei and were counted as apoptotic cells (bright blue fluorescence), *dark blue nuclei were counted as non-apoptotic cells. B) The fold change of apoptotic cells relative to control. The values are the mean of two independent experiments with 100 cells counted under each condition and experiment. Statistically significant, ANOVA, t-test, * p ≤ 0.05 vs control, and # p ≤ 0.05 vs cisplatin*

3.4 Xanthohumol Induces Phosphorylation of H2AX

Histone protein H2AX belongs to the 2A histone family and is rapidly phosphorylated at Ser-139 (γH2AX) in response to DNA damage [21]. Activated γH2AX forms nuclear foci at the sites of DNA damage [22]. To further determine genotoxic effect of xanthohumol, we investigated γH2AX nuclear foci formation using antibodies against phosphorylated H2AX. Immuno - histochemistry analysis showed xanthohumol induced the formation of nuclear γH2AX foci (Fig. 5d-h; green fluorescent dots). Xanthohumol at 6.25 µM minimally induced the formation of γH2AX foci, whereas at 12.5 and 25 µM, xanthohumol strongly induced γH2AX foci formation (Fig. 5f-h). Cisplatin at 25 µM robustly induced γH2AX foci formation. The combination of

cisplatin (25 µM) and 6.25 µM of xanthohumol weakly potentiated γH2AX foci formation (Fig. 5l), whereas at higher xanthohumol concentrations (12.25 and 25 µM) cisplatin potentiated xanthohumol γH2AX foci formation (Fig. 5n-p).

(A)

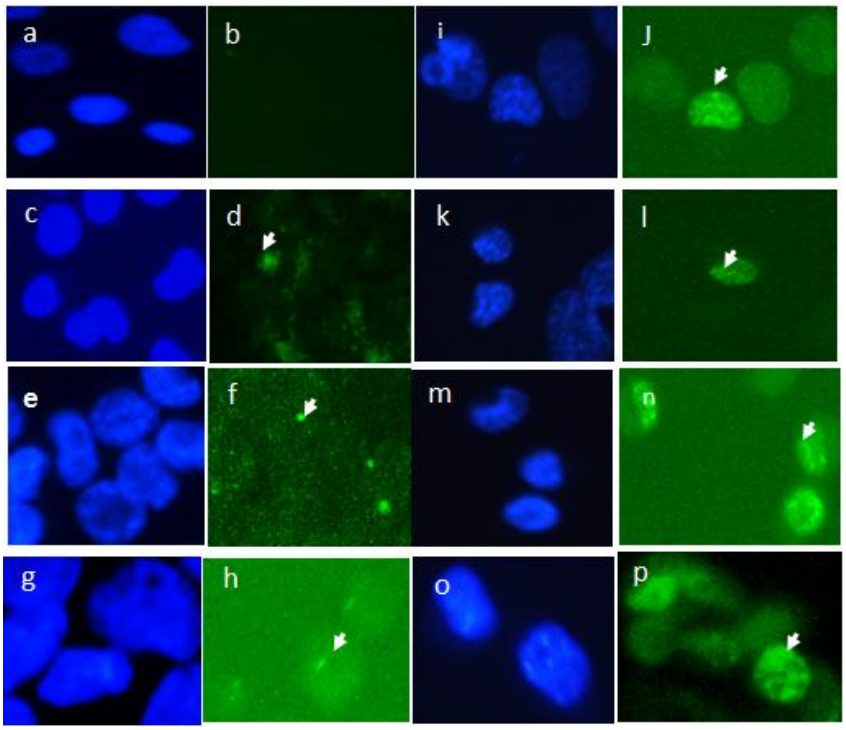

(B)

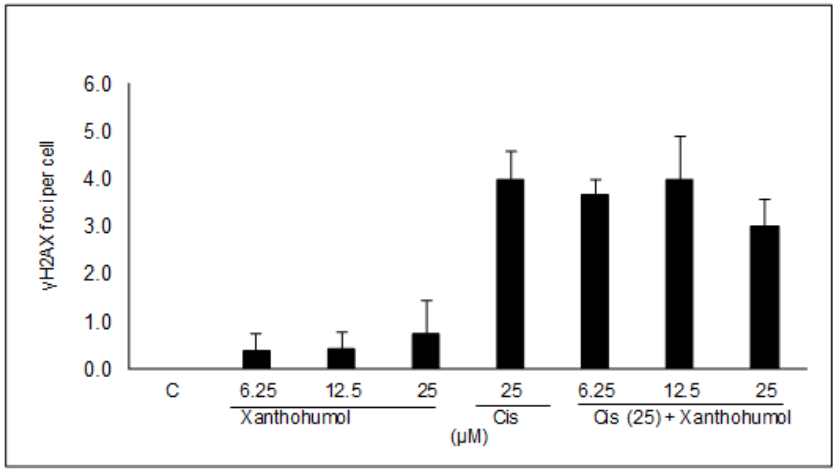

Fig. 5. Xanthohumol induces γH2AX phosphorylation

The cells were cultured on cover slips overnight and then treated with xanthohumol (6.25, 12.5, or 25 µM; d-h), cisplatin (25 µM, j), or combination of cisplatin (25 µM) and xanthohumol (6.25, 12.5, or 25 µM; l-p) for 24 h. After treatments, the cells were washed, fixed, and incubated with primary antibody against phosphorylated γH2AX (green fluorescence) and analyzed as described in Materials and Methods. Nuclei were counter-stained with 4,6 diamidino-2-phenylindole (DAPI, blue fluorescence). Representative micrograph showing γH2AX foci formation (arrow). B. The number of γH2AX foci formation after treatments as shown in A. The data is presented mean ± SEM. The number of foci (green fluorescence) in each cell were counted. Three independent experiments were performed

(A)

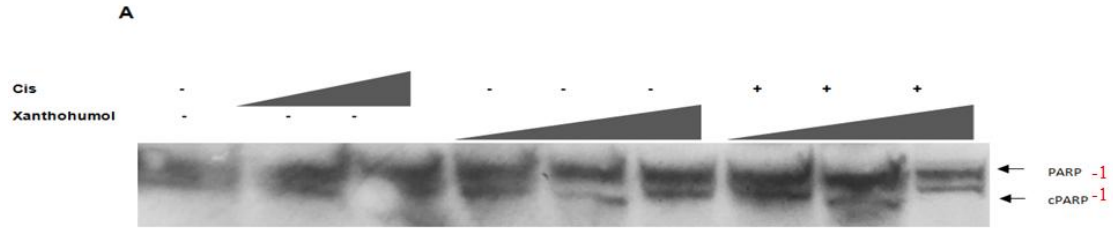

(B)

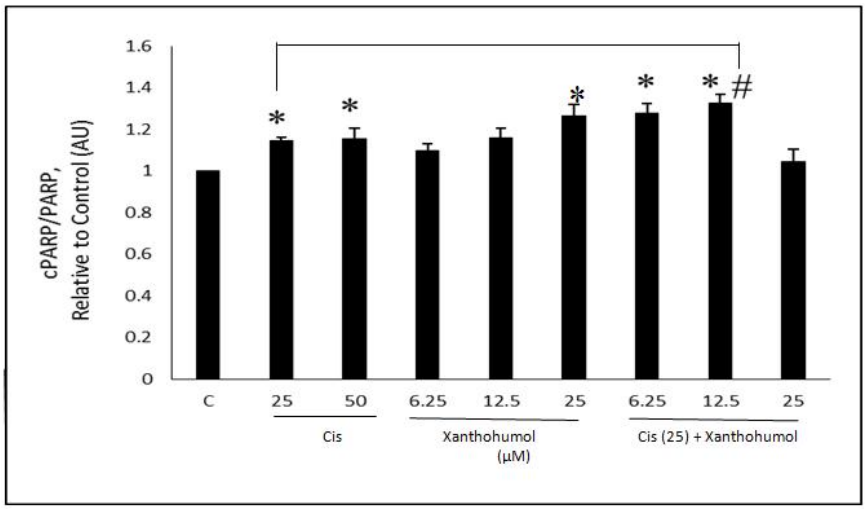

Fig. 6. Xanthohumol induces cPARP-1

*The cells were cultured in growth media for 24 h then treated with cisplatin (25 or 50 μM), xanthohumol (6.25, 12.5 or 25 μM) and the combination of cisplatin (25 μM) and xanthohumol for 24 h. After the treatment, the cells were lysed and the cell lysate was subjected to Western blot analysis as descried in Materials and Methods. A) One representative blot is shown. B) Relative level of cPARP-1 to PARP-1 and control samples, n = 3. Statistically significant, ANOVA, t-test, * p ≤ 0.05 vs control, and # p ≤ 0.05 vs cisplatin*

3.5 Xanthohumol Cleaves PARP-1

To further determine cytotoxic effects of cisplatin (25 or 50 μM), xanthohumol (6.25, 12.5, or 25 μM), and the combination of cisplatin (25 μM) and xanthohumol (6.25, 12.5, or 25 μM), we used Western blot to analyze the level of cleaved (c) PARP-1 (Fig. 6). Cisplatin at both tested concentrations (25 and 50 μM) significantly increased the level of cPARP-1 compared to control. Xanthohumol alone only at 25 μM significantly increased cPARP-1 level compared to control (Fig. 6B). The combination of cisplatin and 6.25 or 12.5 μM of xanthohumol significantly increased cPARP-1 level compared to control (Fig. 6B). The combination of cisplatin and 12.5 μM significantly increased cPARP-1 level compared to cisplatin alone (Fig. 6B).

3.6 Xanthohumol Activates Caspase-3

To further investigate the mechanism by which xanthohumol reduces cell viability, human active caspase-3 (mg/g protein) was measured. The cells were treated with 6.25, 12.5 and 25 μM xanthohumol, 25 μM cisplatin, and the combination of 25 μM cisplatin and xanthohumol (6.25, 12.5 and 25 μM), and active caspse-3 was measured using an ELISA kit (Invitrogen). Xanthohumol only at 12.5 μM significantly increased the level of active capase-3 compared to control (Fig. 7). The addition of 25 μM of cisplatin to all tested concentrations of xanthohumol (6.25, 12.5, or 25 μM) significantly increased the level of active caspase-3 compared to control (Fig. 7). Cisplatin effect on active caspase-3 was significantly potentiated

only by 6.25 μM of xanthohumol compared to cisplatin alone (Fig. 7).

3.7 Xanthohumol Induces $p21^{WAF1/CIP1}$ and $p14^{ARF}$ mRNA Expression

To further determine anti-proliferative effect of xanthohumol by inducing cell cycle arrest genes, we performed qPCR for cell cycle control genes $p21^{WAF1/CIP1}$ and $p14^{ARF}$. Treatment of cells with 12.5 μM of xanthohumol for 24h did not result in a significant increase in $p21^{WAF1/CIP1}$ or $p14^{ARF}$ mRNA (Fig. 5). Whereas a higher concentration of xanthohumol (25 μM) significantly increased $p21^{WAF1/CIP1}$ by 3.31-fold and $p14^{ARF}$ by 1.47-fold increase vs control (Fig. 8, $p \leq 0.05$).

4. DISCUSSION

In this study, we show that xanthohumol induces apoptosis in metastatic lung cancer cells. Moreover, we also found that xanthohumol potentiates cisplatin apoptotic effects. Although new therapies for the treatment of lung cancer have evolved, NSCLC accounts for 85% of lung cancer cases and more than half of the cases are already metastatic at diagnosis [24]. While the treatment options and approaches for malignant lung cancer have evolved significantly, other factors such as secondary resistance is often associated with poor treatment successes and survival [24-25]. Platinum-based chemotherapy including cisplatin in combination with other chemodrugs still remains first line of treatment and has been shown to improve overall survival (OS) in comparison with other drugs such as carboplatin or newer chemodrugs [1,26]. Given cisplatin's efficacy in improving OS in metastatic lung cancer patients, we investigated whether plant-based extract xanthohumol potentiates cisplatin's effects on metastatic lung cancer cells. Xanthohumol exerts antiproliferative effects on various cancer cell lines [27-29]. Bartmanska et al. [27] reported that xanthohumol was more potent than cisplatin against five different cancer cell types. In the present study, we show that xanthohumol was cytotoxic against metastatic lung cancer H1299 cells and its combination with cisplatin enhanced cytotoxic effects compared to each drug alone overall. Addition of xanthohumol to cisplatin (25 μM) significantly decreased cell viability compared to cisplatin alone. Xanthohumol has been shown to decrease viability of different cancer cell lines and induce cellular responses at concentrations that varied from 0.1 μM to 100 μM depending on cell type and exposure time [16,30-31]. In the present study, we tested three concentrations of xanthohumol and although cell viability was significantly decreased at the lowest tested dose of 6. 25 μM, our results are in agreement with those by Yong et al. [16] where xanthohumol decreased A549 cell viability in a dose- and time-dependent manner with an IC_{50} of 74 μM at 24 h. However, another study by Lee et al. [31] reported a much lower IC_{50} of 12.14 μM of xanthohumol on A549 cells viability. Although our viability data shows significant decrease of cell viability at the lowest tested dose, other biological responses showed significant effect at a dose much higher than 6.25 μM. Our results clearly indicate that xanthohumol is cytotoxic to metastatic lung cancer H1299 cells. Cell morphology analysis showed typical cell death traits such as cell shrinkage, loss of cell-cell contact and detachment, and the formation of cytoplasmic vacuoles. Similarly, cisplatin also induced vacuolization. Cytoplasmic vacuolization has been marked with cell death in the presence of a cytotoxic agent [32-34]. Our cell viability results are in agreement with cell morphology data suggesting cell death induced by xanthohumol. To further investigate the mechanism by which xanthohumol induces cell death, we analyzed the state of chromatin condensation and apoptotic bodies formation. Hoechst 33289 binds to condense chromatin and fluoresce brightly which is a hall mark of apoptotic nuclei [35]. Our results demonstrate that xanthohumol alone induced chromatin condensation and its addition to cisplatin potentiated cisplatin's chromatin condensation effect.

To further understand xanthohumol-induced nuclear condensation, we investigated H2AX histone protein phosphorylation at Ser 139 (γH2AX). γH2AX is recruited to the sites of DNA double-strand breaks (DSBs) and participates in chromatin decondensation and plays a role in the initiation of DNA damage repair [36-38]. In the present study, xanthohumol in a dose-dependent manner induced H2AX phosphorylation and γH2AX foci formation within nucleus compared to untreated cells which showed no γH2AX foci formation. The pattern of γH2AX foci formation was distinct for each treatment type. Under xanthohumol treatment alone, the number γH2AX foci per cell was much lower compared to cisplatin. Cisplatin alone induced a greater number of γH2AX within the nucleus of a cell which also displayed a distinct foci pattern such as they were numerous, smaller, and mostly less distinct. When the cells were treated with the

combination of cisplatin and xanthohumol, the number of γH2AX foci was higher than with xanthohumol alone and the foci appeared larger than with cisplatin alone. Our results are consistent with other studies which show that morphological appearance of γH2AX foci is dependent on the type of DNA damage induced by different agents [36-38]. Sears et al. [38] showed γH2AX foci formation in lung cancer cells in response to cisplatin-induced DNA damage. In the present study, cisplatin-induced foci are consistent with those by Sears et al. [38]. However, the pattern of γH2AX formation in response to xanthohumol appeared distinct from those induced by cisplatin suggesting that xanthohumol induces DNA damage most likely by a mechanism that still remains to be determined.

A hallmark of DNA damage is the formation of γH2AX foci within nucleus and activation of PARP-1 and other repair factors [39-40]. Although PARP-1 plays a role in DNA repair, its cleavage by activated caspases leads to the formation of cleaved(c)-PARP-1, a hallmark of apoptosis [40-42]. In the present study, Western blot analysis showed an increased c-PARP-1 level in cells lysates treated with cisplatin, xanthohumol at 25 μM and the combination of cisplatin and 6.25 or 12.5 μM of xanthohumol. Cleavage of PARP-1 is mediated by caspases and considered a hallmark of apoptosis [42]. While almost all caspases cleave PARP-1, caspase-3 has been shown to cleave PARP *in vitro* and *in vivo* [43-44]. Our results indicate 12.5 μM of xanthohumol, cisplatin, and combination of cisplatin with xanthohumol increased active caspase-3 above control level. Addition of 6.25 μM of xanthohumol potentiated cisplatin-induced active caspase-3 level. Increased activity of caspase-3 by xanthohumol has been previously reported on lung adenocarcinoma A549 with concentration of 28 μM [16]. Although in our study we report 12.5 μM xanthohumol increasing active capase-3 which is lower than those reported by Yong et al. [16], the difference might be due to different cell types. Previous studies showed that caspase-3 is primarily responsible for cleavage of PARP-1 during cell death [38-39]. In the present study, the difference of one order of magnitude of xanthohumol necessary to increase cPARP-1 level and active casapase-3 suggests that cleavage of PARP-1 follows activation of caspase-3.

PAPR-1 cleavage and phosphorylation of γH2AX occurs in response to DNA damage [28, 41, 45-46]. γH2AX also plays a role in p53/p21 pathway

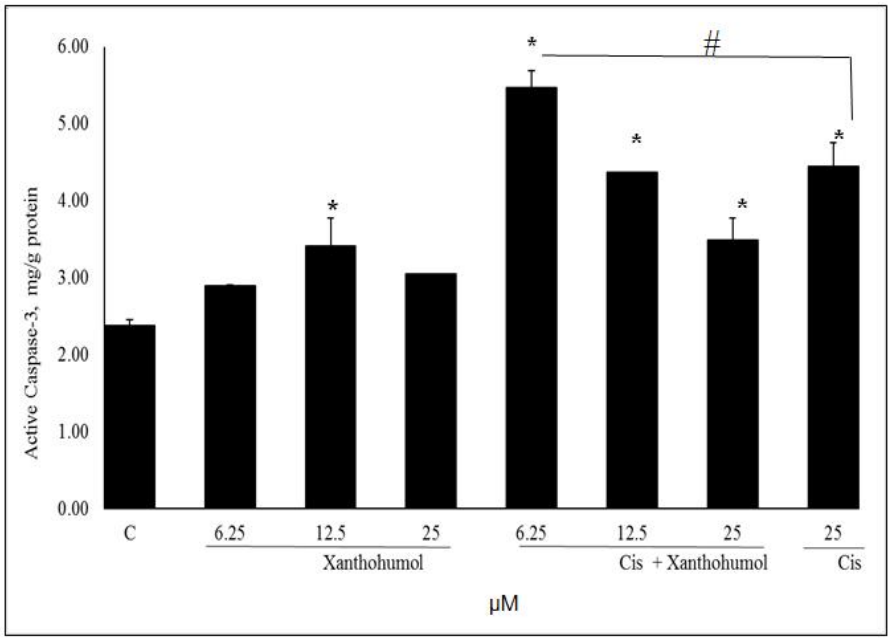

Fig. 7. Xanthohumol activates caspase-3

*The cells were cultured in % growth media for 24 h and then treated with xanthohumol (6.25, 12.5 and 25 μM), cisplatin (25 μM), or combination of cisplatin and xanthohumol for 24 h. After the treatment, the cells were lysed, and cell lysate was subjected to caspase 3 assay as descried in Materials and Methods. The data represents the mean ± SEM, n = 4. Statistically significant, ANOVA, t-test, * p ≤ 0.05 vs control, and # p ≤ 0.05 vs cisplatin*

(A)

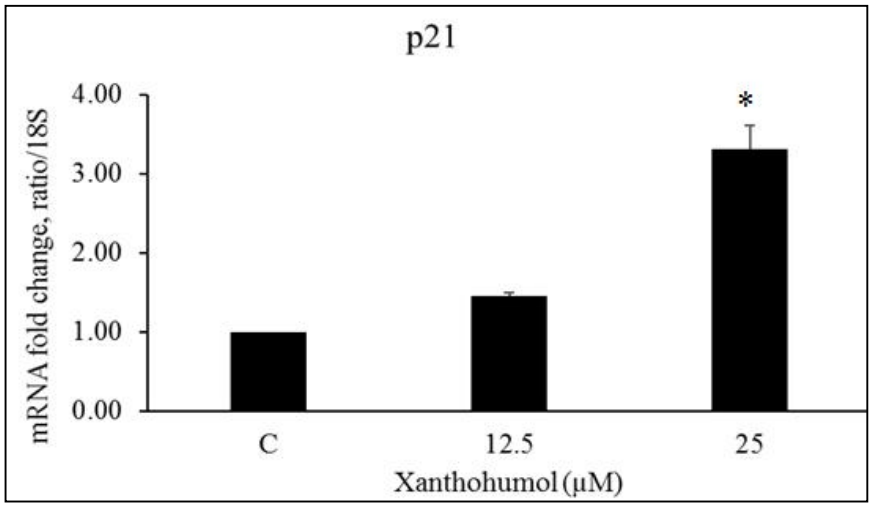

(B)

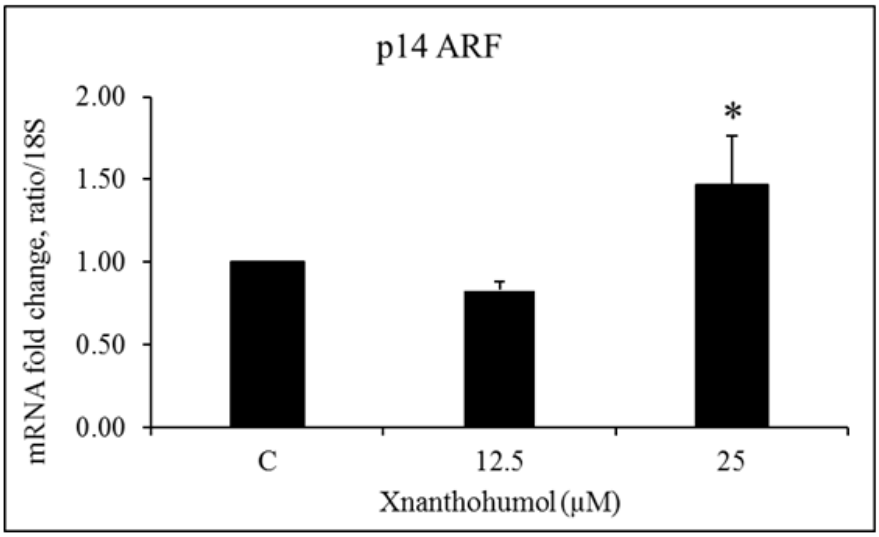

Fig. 8. Regulation of $p21^{WAF1/CIP1}$ (A) and $p14^{ARF}$ (B) mRNA

*The cells were seeded in growth media for 24 h followed by treated with xanthohumol (12.5 or 25 µM) in basal media for an additional 24 h. After the treatment, the cell monolayer was rinsed with PBS and total RNA was isolated and qPCR were performed as described in Materials and Methods. The data is presented as mRNA fold change relative to 18S. The data represents the mean ± SEM, n = 4. *Statistically significant, ANOVA, t-test, p ≤ 0.05 vs control*

and is required in the p21-induced cell cycle arrest [47]. Role of $p21^{WAF1/CIP1}$ and $p14^{ARF}$ in arresting cell growth and induction of apoptosis has been previously reported [48-50]. In the present study xanthohumol increased $p21^{WAF1/CIP1}$ and $p14^{ARF}$ mRNA. These data suggest that xanthohumol regulates cell cycle progression thus limiting metastatic lung cancer cell growth.

Cisplatin still remains first line of chemotherapy for NSCLC even as survival remains low [51]. In the present study we show that combination of cisplatin and xanthohumol reciprocally potentiated each other's cytotoxic effect on metastatic lung cancer H1299 cells by decreasing cell viability, inducing chromatin condensation, H2AX phosphorylation, increasing cPARP-1 and active caspase-3, and cell cycle progression control genes $p21^{WAF1/CIP1}$ and $p14^{ARF}$. Cisplatin crosslinks DNA and inhibits DNA replication, however chemosenstivity to cisplatin is impeded by chemoresistance, and the results of our study suggest that xanthohumol

may potentiate cisplatin antigrowth effects on metastatic lung cancer cells in an overlapping and distinct mechanisms. While both compounds induced the formation of γH2AX foci, the pattern of these foci were distinct between the two compounds.

5. CONCLUSION

In conclusion, our data indicate that combining cisplatin with xanthohumol led to reciprocal potentiation of their separate anticancer properties and points to a possibly new drug combination for targeting metastatic lung cancer.

CONSENT

It is not applicable.

ETHICAL APPROVAL

It is not applicable.

FUNDING

This work was supported by NIH/NIGMS Grant No. R25GM067122 through RISE at Jackson State University and by Jackson State University President's Creative Award.

ACKNOWLEDGEMENT

We thank Dr. Kristine Krajnak and Dr. Victor Ogungbe for reading the manuscript and minor suggestions.

COMPETING INTERESTS

Authors have declared that no competing interests exist.

REFERENCES

1. Ardizzoni A, Boni L, Tiseo M, Fossella FV, Schiller JH, Paesmans M, et al. Cisplatin-versus carboplatin-based chemotherapy in first-line treatment of advanced non-small-cell lung cancer: An individual patient data meta-analysis. J Natl Cancer Inst. 2007;99:847-857.
2. Siegel RL, Miller KD, Ahmeding J. Cancer Statistics. CA Cancer J Clin. 2016;66:7-30.
3. Shankar A, Dubey A, Saini D, Singh M, Prasad CP, Shubham R, et al. Environmental and occupational determinants of lung cancer. Transl Lung Cancer Res. 2019;S31-S49.
4. Reck M, Heigener DF, Mok T, Soria JC, Rabe KF. Management of non-small-cell lung cancer: recent developments. Lancet. 2013;382:709-719.
5. Peters S, Adjei AA, Gridelli C, et al. Metastatic non-small-cell lung cancer (NSCLC): ESMO Clinical Practice Guidelines for diagnosis, treatment and follow-up. Ann Oncol. 2012;23:56-64.
6. Mi S, Xiang G, Yuwen D, Gao J, Guo W, Wu X, Sun Y, Su Y, Shen Y, Xu Q. Inhibition of autophagy by andrographolide resensitizes cisplatin-resistant non-small cell lung carcinoma cells via activation of the Akt/mTOR pathway. Toxicol Appl Pharmacol. 2016;310:78-86.
7. Peng DJ, Wang J, Zhou JY, Wu GS. Role of the Akt/mTOR survival pathway in cisplatin resistance in ovarian cancer cells. Biochem Biophys Res Commun. 2010;394:600-605.
8. Oh IJ, Kim KS, Park CK, Kim YC, Lee KH, Jeong JH, Kim SY, Lee JE, Shin KC, Jang W, Lee HK, Lee KY, Lee SY. Belotecan/cisplatin versus etoposide/cisplatin in previously untreated patients with extensive-stage small cell lung carcinoma: A multi-center randomized phase III trial. BMC Cancer. 2016;201:690.
9. Elkady AI, Ramadan WS. The aqueous extract of cinnamon bark ameliorated cisplatin-induced cytotoxicity in vero cells without compromising the anticancer efficiency of cisplatin. Biomed Pap Med Fac Palacky Olomouc Czech Repub. 2016;160:363-71.
10. Jiang CH, Sun TL, Xiang DX, Weis SS, Li WQ. Anticancer activity and mechanisms of zanthohumol: A prenylated flavonoid from hops (*Humulus lupulus* L.). Front Pharmacol. 2018; 9:530.
11. Liu M, Hansen PE, Wang G, Qiu L, Dong J, Yin H, Qian Z, Yang M, Miao J. Pharmacological profile of xanthohumol, a prenylated flavonoid from hops (*Humulus lupulus*). Molecules. 2015;20:754-779.
12. Venturelli S, Burkard M, Biendl M, Lauer UM, Frank J, Busch C. Prenylated chalcones and flavonoids for the prevention and treatment of cancer. Nutrition. 2016;8:32:1171-1178.
13. Slawinska-Brych A, Zdzinska B, Dmoszynska-Graniczka M, Jeleniewicz W, Kurzepa J, Gagos M, Stepulak A. Xanthohumol inhibits the extracellular

signal regulated kinase (ERK) signaling pathway and suppresses cell growth of lung adenocarcinoma cells. Toxicology. 2016;357-358:65-73.

14. Slawinska-Brych A, Zdzinska B, Czerwonka A, Mizerska-Kowalska M, Dmoszynska-Graniczka M, Stepulak A, Gagos M. Xanthohumol exhibits anti-myeloma activity in vitro through inhibition of cells proliferation, induction of apoptosis via the ERK and JNK-dependent mechanism and suppression of sIL-6R and VEGF production. Biochim Biophys Acta Gen Subj. 2019;1863:129408.
15. Sastre-Serra J, Ahmiane Y, Roca P, Oliver J, Pons DG. Xanthohumol, a hop-derived prenulflavonoid present in beer, impairs mitochondrial functionality of SW620 colon cancer cells. Int J Food Sci Nutr. 2019;70: 396-404.
16. Yong WK, Ho YF, Malek SN. Xanthohumol induces apoptosis and S phase cell cycle arrest in A549 non-small cell lung cancer cells. Pharmacogn Mag. 2015;11:S275-283.
17. Li J, Ye T, Liu Y, Kong L, Sun XZ, Liu D, Wang J, Xing HR. Transcriptional activation of Gstp1by MEK/ERK signaling confer chemo-resistance to cisplatin in lung cancer stem cell. Front Onclol. 2019; 9:476.
18. Kunnimalaiyann S, Sokolowski KM, Balamurugan M, Gamblin TC, Kunnimaliyaan M. Xanthohumol inhibits Notch signaling and induces apoptosis in hepatocellular carcinoma. PLoS One. 2015;10:e0127464.
19. Pacurari M, Qian Y, Porter DW, Wolfarth M, Wan Y, Luo D, Ding M, Castranova V, Guo NL. Multi-walled carbon nanotube-induced gene expression in the mouse lung: Association with lung pathology. Toxicol Appl Pharmacol. 2011; 255:18–31.
20. Pacurari M, Addison BJ, Bondalapati N, Wan YW, Luo D, Qian Y, Castranova V, Ivanov AV, Guo NL. The microRNA-200 family targets multiple non-small cell lung cancer prognostic markers in H1299 cells and BEAS-2B cells. Int J Oncol. 2013;43:548–560.
21. Rogakou EP, Pilch DR, Orr AH, Ivanova VS, Bonner WM. DNA double stranded breaks induce histone H2AX phosphorylation on serine 139. J Biol Chem. 1998;273:5858–5868.
22. Riches LC, Lynch AM, Gooderham NJ. Early events in the mammalian response to DNA double-strand breaks. Mutagenesis. 2008;23;331–339.
23. Pacurari M, Yin XJ, Zhao J, et al. Raw single-wall carbon nanotubes induce oxidative stress and activate MAPKs, AP-1, NF-kappaB, and Akt in normal and malignant human mesothelial cells. Environ. Health Perspect. 2008;116:1211–1217.
24. Chou HL, Lin YH, Liu W, Wu CY, Li RN, Huang HW, Chou CH, Chiou SH, Chiu CC. Combination therapy of chloroquine and C2-ceramide enhances cytotoxicity and lung cancer H460 and H1299 cells. Cancers. 2019;11:370.
25. Heigener DF, Kerr KM, Laing GM, Mok TSK, Moiseyenko FV, Reck M. Redefining treatment paradigms in first-line advanced non-small cell lung cancer. Clinical Cancer Research; 2019;
DOI: 10.1158/1078-0432.CCR-18-1894.
26. Reck M, Popat S, Reinmuth N, Ruysscher DD, Kerr KM, Peters S. Metastatic non-small -cell lung cancer (NSCLC): ESMO clinical practice guidelines for diagnosis treatment and follow-up. Annals of Oncology. 2004;25:27-39.
27. Bartmanska A, Tronina T, Poplonski J, Milczarek M, Filip-Psurska B, Wietrzyk J. Highly cancer selective antiproliferative activity of natural prenylated flavonoids. Molecules. 2018;23:E2922.
28. Guo D, Zhang B, Liu S, Jin M. Xanthohumol induces apoptosis via caspase activation, regulations of Bcl-2, and inhibition of PI3K/Akt/mTOR-kinase in human gastric cancer cancer cells. Biome Pharmacother. 2018;1300-1306.
29. Jiang CH, Sun TL, Xiang DX, Weis SS, Li WQ. Anticancer activity and mechanisms of zanthohumol: A prenylated flavonoid from hops (*Humulus lupulus* L.). Front Pharmacol. 2018; 9:530.
30. Strathmann J, Gerhauser C. Anti-proliferative and apoptosis-inducing properties of xanthohumol, a prenylated chalcone from hops (*Humulus lupulus* L.) In: Diederich M, Noworyta K, editors. Natural Compounds as Inducers of Cell Death. Netherlands: Springer; 2012;69–93.
31. Lee SH, Kim HJ, Lee JS, Lee IS, Kang BY. Inhibition of topoisomerase I activity and efflux drug transporters' expression by

xanthohumol from hops. Arch Pharm Res. 2007;30:1435-1439.
32. Foo NC, Ahn BY, Ma X, Hyun W, Yen TSB. Cellular vacuolization and apoptosis induced by hepatitis B virus large surface protein. Hepatology. 2002;36:1400-1407.
33. Shubin AV, Demidyuk IV, Komissarov AA, Rafieva LM, Kostrov SV. Cytoplasmic vacuolization in cell death and survival. Oncotarget. 2016;7:55863-55889.
34. Kuo LJ, Yang LX. Gamma-H2AX - A novel biomarker for DNA double-strand breaks. In Vivo. 2008;22:305-309.
35. Li Y, Pan J, Gou M. The anti-proliferation, cycle arrest and apoptotic inducing activity of peperomin E on prostate cancer PC-3 cell line. Molecules. 2019;24:1472.
36. Singha PK, Pandeswara S, Venkatachalam MA, Saikumar P. Manumycin a inhibits triple-negative breast cancer growth through LC3-mediated cytoplasmic vacuolation death. Cell Death Dis. 2013;4:e457.
37. Revet I, Feeney L, Bruguera S, Wilson W, Dong TK, Oh DH, Dankort D, Cleaver JE. Functional relevance of the histone gammaH2Ax in the response to DNA damaging agents. Proc Natl Acad Sci U S A. 2011;108:8663-8667.
38. Sears CR, Cooney SA, Chin-Sinex H, Mendonca MS, Turchi JJ. DNA Damage Response (DDR) pathway engagement incisplaitn radiosensitization of non-small cell lung cancer. DNA repair (Amst). 2016;40:35-46.
39. Nicholson DW, Ali A, Thornberry NA, Vailla ncourt JP, Ding CK, Gallant M, et al. Identification and inhibition of the ICE/CED-3 protease necessary for mammalian apoptosis. Nature. 1995;376:37–43.
40. Tewari M, Quan LT, O'Rourke K, Desnoyer s S, Zeng Z, Beidler DR, et al. Yama/ CPP32 beta, a mammalian homolog of CED-3, is a CrmA-inhibitable protease that cleaves the death substrate poly(ADP-ribose) polymerase. Cell. 1995;801-809.
41. Le Rhun Y, Kirkland JB, Shah GM. Cellular responses to DNA damage in the absence of Poly(ADP-ribose) polymerase. Biochem Biophys Res Commun. 1998;245:1-10.
42. Wang M, Wu W, Wu W, Rosidi B, Zhang L, Wang H, Iliakis G. PARP-1 and Ku compete for repair of DNA double strand breaks by distinct NHEJ pathways. Nucleic Acids Res. 2006; 34:6170-6182.
43. Kaufmann SH, Desnoyers S, Ottaviano Y, Davidson NE, Poirier GG. Specific proteolytic cleavage of poly(ADP-ribose) polymerase: an early marker of chemotherapy-induced apoptosis. Cancer Res. 1993;53:3976-3985.
44. Lazebnik YA, Kaufmann SH, Desnoyers S, Poirier GG, Earnshaw WC. Cleavage of poly(ADP-ribose) polymerase by a proteinase with properties like ICE. Nature. 1994;371:346-7.
45. Downey M, Durocher D. γH2AX as a checkpoint maintenance signal. Cell Cycle. 2006;5: 1376-1381.
46. Fragkos M, Jurvansuu J, Beard P. H2Ax is required or cell cycle arrest via the p53/p21 pathway. Mol Cell Biol. 2009;29:2028-40.
47. Hustedt N, Durocher D. The control of DNA repair by the cell cycle. Nature Cell Biology. 2016; 19:1-9.
48. Eymin B, Leduc C, Coll JL, Brambilla E, Gazzeri S. p14ARF induces G2 arrest and apoptosis independently of p53 leading to regression of tumors established in nude mice. Oncogene. 2003;22:1822-1835.
49. Kim M, Sgagias M, Deng X, Jung YJ, Rikiyama T, Lee K. Apoptosis induced by adenovirus-mediated p14ARF expression in U2OS osteosarcoma cells is associated with increased Fas expression. Biochem Biophys Res Commun. 2004;320:138-144.
50. Taguchi T, Kato Y, Baba Y, Nishimura G, Tanigaki Y, Horiuchi C. Protein levels of p21, p27, cyclin E and Bax predict sensitivity to cisplatin and paclitaxel in head and neck squamous cell carcinomas. Oncol Rep. 2004;11:421-426.
51. Stinchcombe TE, Socinski MA. Current treatments for advanced stage non-small cell lung cancer. Proc Am Thorac Soc. 2009;6(2):233-41.

Peer-review history:
The peer review history for this paper can be accessed here:
https://sdiarticle4.com/review-history/50994